Regional Quantitative DCE-MRI in the pancreas

J. H. Naish[1], C. E. Hutchinson[1], Z. Esmail[2], Y. Watson[1], S. Cheung[1], D. M. McGrath[1], J. C. Waterton[1,3], P. D. Hockings[4], C. J. Taylor[1], and G. J. Parker[1]

[1]Imaging Science and Biomedical Engineering, University of Manchester, Manchester, United Kingdom, [2]University of Salford, Salford, United Kingdom, [3]AstraZeneca, Macclesfield, United Kingdom, [4]AstraZeneca, Mölndal, Sweden

INTRODUCTION

The islets of Langerhans, which form the functional units of the endocrine pancreas, comprise 1-2% of the mass of the pancreas. An ability to monitor the islets would be of great benefit to research into both type 1 and type 2 diabetes mellitus but since each islet is of order 0.1-0.2mm across they are not amenable to direct in-vivo visualisation by MRI. The islets are highly vascularised and receive 10-15% of the total blood supply to the pancreas, such that functional MRI methods may offer a valuable non-invasive probe of the islet microvasculature. Recently, changes in islet microvasculature associated with inflammation in a murine model of type 1 diabetes has been observed using MRI of magnetic nanoparticles (1). The main aim of the present study was to assess the feasibility of quantitative tracer kinetic model-based DCE-MRI in the pancreas in human volunteers. An additional aim was to investigate the sensitivity of the derived kinetic parameters to location in the pancreas by comparing regions of interest in the pancreatic tail to regions of interest in the pancreatic head.

METHODS

Subjects A group of 9 non-diabetic volunteers were recruited (6 female, age 26-54). The study was approved by the Local Research Ethics Committee and all subjects gave written informed consent. Subjects fasted for a minimum of 3 hours prior to imaging.

Image Acquisition Imaging was carried out using a Philips 1.5T Intera system (Philips Medical Systems, Best, NL). The DCE-MRI protocol consisted of 3D RF-spoiled fast field echo (spoiled gradient echo (GRE)) axial acquisitions with 25 slices, slice thickness 4mm (8mm over-contiguous) , FOV 375x375mm, matrix size 128x128, TR 4.0ms, TE 0.82ms. Baseline T_1 was determined using 4 separate acquisitions prior to the DCE-MRI time series with flip angles of 2°, 4°, 9° and 20° and 4 signal averages. The dynamic series consisted of 75 consecutively acquired volumes with a flip angle of 20°, one signal average and a temporal resolution of 4.9s. Contrast agent was administered intravenously at the beginning of the sixth dynamic volume by power injector. 0.05 mmol/kg of body weight of Omniscan 0.5 mmol/ml (gadodiamide, GE Healthcare) was administered at a rate of 3ml/s followed by an equal volume of saline flush. Prior to the dynamic protocol, anatomical T_1 and T_2-weighted volumes were acquired using the same slice thickness, number of slices, FOV and location as the dynamic series but with an in-plane resolution of 256x256.

Analysis The dynamic series signal intensity was converted to contrast agent concentration using the baseline T_1 calculation and employing the standard relationship between a spoiled GRE acquisition and T_1. Individual subject arterial input functions were obtained from the aorta of each volunteer using an automated extraction method described previously (2). Regions of interest encompassing the head and tail sections of the pancreas were manually defined on each image slice using the high resolution anatomical images. A pharmacokinetic model was fitted to the dynamic data on a voxel-by-voxel basis within the defined 3D ROIs. The model used was an extension to the Kety model (3) $C_t(t) = v_p C_p(t-\omega) + K^{trans}\int_0^t C_p(t'-\omega)\exp\left(-\frac{K^{trans}(t-t')}{v_e}\right)dt'$ where $C_t(t)$ is the concentration of contrast agent in the tissue, C_p is the concentration of contrast agent in the blood plasma, K^{trans} is the volume transfer coefficient, v_p is the blood plasma volume fraction, v_e is the volume fraction of the extravascular extracellular space, and ω is the temporal offset between arterial input function (C_p) and tissue uptake curve (C_t).

The area under the first 60s of the contrast agent concentration curve (IAUC60) was also calculated on a voxel-by-voxel basis.

Statistical analysis The median value for each parameter within each head or tail ROI for each subject was calculated. Parameter values in the head versus the tail were compared after log transformation using a paired t-test and confidence intervals were back transformed. The decision to transform the data was made following the observation that K^{trans}(tail)-K^{trans}(head) scaled with mean K^{trans}.

RESULTS

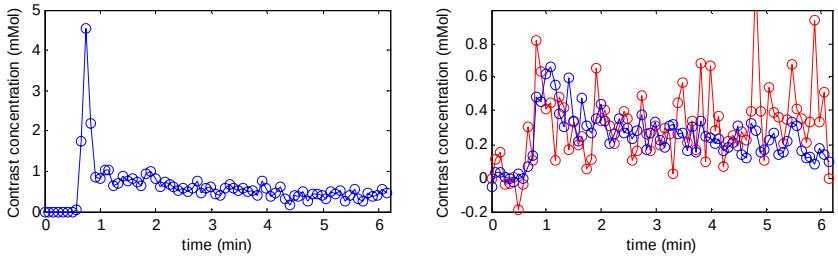

Figure 1 *a) Example AIF automatically extracted from the aorta b) Example contrast agent uptake curves taken from small ROIs in the head (blue) and tail (red) of the pancreas*

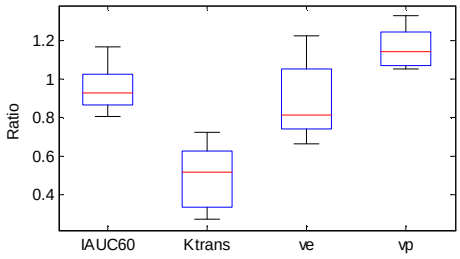

Figure 2 *Box-plots of the ratio of median parameters across tail ROI to head ROI*

An example AIF extracted automatically from the aorta is presented in figure 1a and example uptake curves taken from small regions of interest (approx 10 voxels) placed in the pancreas head and tail are presented in figure 1b. Median values for IAUC60, K^{trans}, v_e and v_p averaged across the 9 subjects are presented in Table 1 together with results of the statistical analysis. Box-plots of the ratio of kinetic parameters measured in the tail ROI to those in the head ROI are presented in figure 2.

The uptake curves are noisy but differences in the form of the curves could be observed between the head and tail in that the contrast uptake peaked more sharply in the tail and was less sustained than in the head (see figure 1b). This qualitative difference is reflected in the kinetic parameters. K^{trans} was significantly and consistently lower in the tail when compared with the head and v_p was significantly and consistently higher. There were no statistically significant differences in IAUC60 or v_e.

	Head	**Tail**	**Ratio of tail to head**	
	Mean(SD)	**Mean(SD)**	**Mean (CI)**	**P value**
IAUC60	18.0 (4.4)	16.7 (3.3)	0.95 (0.86, 1.03)	0.2
K^{trans}	0.41 (0.18)	0.19 (0.10)	0.50 (0.36, 0.62)	**0.0002**
v_e	0.21 (0.09)	0.19 (0.09)	0.88 (0.72, 1.01)	0.07
v_p	0.13 (0.03)	0.15 (0.04)	1.17 (1.09, 1.25)	**0.0006**

Table 1 *Mean across subjects of median values for kinetic parameters in head and tail ROIs and results of the statistical analyses. IAUC60 is measured in mmol.s, K^{trans} in ml/min/ml.*

DISCUSSION AND CONCLUSION

The observation of significantly lower K^{trans} in the tail regions may indicate lower flow or lower permeability in this region but since the pancreas is generally vascular, it is less likely that K^{trans} is flow-limited and our results may be suggesting a lower permeability of the capillaries in the tail. The observed higher blood volume (v_p) may indicate increased vasculature towards the tail. These observations may reflect structural differences between the head and tail regions possibly resulting from the different embryonic origins. In conclusion, this study has demonstrated the feasibility of DCE-MRI in the pancreas which, by fitting a tracer kinetic model, is sensitive to regional differences in microvasculature. The technique may benefit studies of type 1 and type 2 diabetes. **REFERENCES** (1) Turvey SE et al, *J Clin Invest* **115**:2454–2461 (2005). (2) Parker GJM et al, *Magn Reson Med*, **56**, 993-1000 (2006). (3) Daldrup HE et al, *Magn Reson Med* **40**, 537-543 (1998).

Acknowledgements The study was funded by AstraZeneca.